



Open Access This file is licensed under a Creative Commons Attribution 4.0 International License, which permits use, sharing, adaptation, distribution and reproduction in any medium or format, as long as you give appropriate credit to the original author(s) and the source, provide a link to the Creative Commons license, and indicate if changes were made. In the cases where the authors are anonymous, such as is the case for the reports of anonymous peer reviewers, author attribution should be to 'Anonymous Referee' followed by a clear attribution to the source work. The images or other third party material in this file are included in the article's Creative Commons license, unless indicated otherwise in a credit line to the material. If material is not included in the article's Creative Commons license and your intended use is not permitted by statutory regulation or exceeds the permitted use, you will need to obtain permission directly from the copyright holder. To view a copy of this license, visit <http://creativecommons.org/licenses/by/4.0/>.

Web links to the author's journal account have been redacted from the decision letters as indicated to maintain confidentiality

11th Sep 23

Dear Dr Mirzaali,

Thank you for submitting your manuscript, "Curvature tuning through defect-based 4D printing", to Communications Materials, and please accept our most sincere apologies for the delay in communicating our decision, due to the scarce availability of reviewers over the summer months. Your manuscript has now been seen by 3 referees, whose comments are appended below. You will see that while they find your work of interest, some important requests for technical details and further explanations are raised. We are interested in the possibility of publishing your study in Communications Materials, but would like to consider your response to these concerns in the form of a revised manuscript before we make a decision on publication.

We therefore invite you to revise and resubmit your manuscript, taking into account the points raised.

We are committed to providing a fair and constructive peer-review process. Please don't hesitate to contact us if you wish to discuss the revision in more detail.

When submitting your revised manuscript, please include the following:

- A response letter with a point-by-point reply to each of the referee comments and a description of changes made. Please include the complete referee report in the response letter. Please note that the response letter must be separate to the cover letter to the editors.
- A marked-up version of the manuscript with all changes to the text in a different colored font. Please do not include tracked changes or comments. Please select the file type 'Revised Manuscript - Marked Up' when uploading the manuscript file to our online system.
- A clean version of the manuscript. Please select the file type 'Article File'.
- An updated <https://www.nature.com/documents/nr-editorial-policy-checklist.zip> Editorial Policy checklist, uploaded as a 'Related Manuscript File' type. This checklist is to ensure your paper complies with all relevant editorial policies. If needed, please revise your manuscript in response to these points. Please note that this form is a dynamic 'smart pdf' and must therefore be downloaded and completed in Adobe Reader. Clicking this link will download a zip file containing the pdf.

In the event that your manuscript is accepted we will provide detailed guidance on our journal policies and formatting. You may however wish to ensure that the manuscript complies with our house style at this stage. See our style and formatting guide (<https://www.nature.com/documents/commsj-phys-style-formatting-guide-accept.pdf>) and checklist (<https://www.nature.com/documents/commsj-phys-style-formatting-checklist-article.pdf>) for reference.

Data availability statements and data citations policy: All Communications Materials manuscripts must include a section titled "Data Availability" at the end of the Methods section or main text (if no

Methods). More information on this policy, and a list of examples, is available at <http://www.nature.com/authors/policies/data/data-availability-statements-data-citations.pdf>.

In particular, the Data availability statement should include:

- Accession codes for deposited data
- Other unique identifiers (such as DOIs and hyperlinks for any other datasets)
- At a minimum, a statement confirming that all relevant data are available from the authors
- If applicable, a statement regarding data available with restrictions
- If a dataset has a Digital Object Identifier (DOI) as its unique identifier, we strongly encourage including this in the Reference list and citing the dataset in the Data Availability Statement.

DATA SOURCES: We strongly encourage authors to deposit all new data associated with the paper in a persistent repository where they can be freely and enduringly accessed. We recommend submitting the data to discipline-specific, community-recognized repositories, where possible and a list of recommended repositories is provided at <http://www.nature.com/sdata/policies/repositories>.

If a community resource is unavailable, data can be submitted to generalist repositories such as [figshare](https://figshare.com/) or [Dryad Digital Repository](http://datadryad.org/). Please provide a unique identifier for the data (for example a DOI or a permanent URL) in the data availability statement, if possible. If the repository does not provide identifiers, we encourage authors to supply the search terms that will return the data. For data that have been obtained from publically available sources, please provide a URL and the specific data product name in the data availability statement. Data with a DOI should be further cited in the methods reference section.

Please refer to our data policies at <http://www.nature.com/authors/policies/availability.html>.

Please use the following link to submit your documents:

[link redacted]

** This url links to your confidential home page and associated information about manuscripts you may have submitted or be reviewing for us. If you wish to forward this email to co-authors, please delete the link to your homepage first **

We hope to receive your revised paper within three months; please let us know if you aren't able to submit it within this time so that we can discuss how best to proceed. If we don't hear from you, and the revision process takes significantly longer, we will close your file. In this event, we will still be happy to reconsider your paper at a later date, as long as nothing similar has been accepted for publication at Communications Materials or published elsewhere in the meantime.

Please do not hesitate to contact me if you have any questions or would like to discuss these revisions further. We look forward to seeing the revised manuscript and thank you for the

opportunity to review your work.

Best regards,

Dr Aldo Isidori
Senior Editor
Communications Materials

Reviewers' comments:

Reviewer #1 (Remarks to the Author):

A new design approach is presented that applies a fused deposition modeling process to create planar structures capable of out-of-plane deformation. By controlling the printing speed and incorporating multi-material printing, it is possible to obtain a variety of shapes covering negative to positive values of mean and Gaussian curvature. This is an interesting work, but some minor issues need to be addressed.

1. A sudden drop (between $h=1.5$ mm and $h=2$ mm) was observed from the β_2 curve in Figure 2b, and a more detailed explanation is needed to elucidate this phenomenon. Furthermore, in Figure 2b, are β_1 and β_2 an average value or were they tested only once?
2. More details about the computational modeling should be shown, especially the input of material parameters (including anisotropic thermal expansion) and loading conditions (temperature) in the temperature-displacement steady-state analysis.
3. Are the material parameters in Tables S1 and S2 the ones actually measured in this study?
4. Was the temperature-dependent elastic moduli of PLA determined by tensile experiments, or was the storage modulus from the DMA used directly as a substitute? If the latter, it is not rigorous.
5. The authors create "imperfections" by setting different printing speeds. Can the inevitable gaps between deposition lines in the FDM process be introduced as "imperfections"?

Reviewer #2 (Remarks to the Author):

This paper utilized the combination of PLA material and other softer materials, and the disc bends into a smooth surface of various curvations by adjusting the area proportion of the two materials. Also, the disc structure can be deformed into a dome structure of different curvations as needed with applying different printing speeds to the two materials in the area. Moreover, the reverse bending disk and the positive bending disk can be combined, such as the structure composed of the dome structure below and the saddle-shaped curved structure above.

1. Only the influence on the change of the proportion of the two materials in the radial direction of the disk on the deformation is discussed, which should be further discussed in the axial direction. For example, the disk is divided into several layers with the same and uniform thickness, and whether the number of layers occupied by the two materials has an influence on the deformation effect should be included. What's more, the influence of different layers occupied by PLA material and TPU material on surface curvature shall be further refined.
2. If it is possible, it's better to further refine the area of the material in the disc, and select a variety of materials to distribute in various proportions in the radial and axial directions of the disc, so that

the disc presents a gradient structure and can be deformed into a more complex curved surface structure with multiple gradients and curvations.

3. In this paper, there is no 3D solid sample successfully printed by this design method for practical application, if it is possible to print a three-dimensional solid structure that realizes functional gradient characteristic utilizing the gradient structure.

Reviewer #3 (Remarks to the Author):

The authors present a methodology coupled with modelling of the deformation of FDM components, including those built from multi-materials. The following minor comments should be taken into account for this manuscript to be further considered.

1. Deformations and stress/strain distributions are influenced by the selected concentric rings printing path. So, what can the authors expect if other printing trajectories are selected?
2. Why did the authors select this printing path?
3. For the multi-material printed samples, In %, how much PLA and TPU were used? Discussion on different multi-material strategies could also enhance the current version, e.g., different materials in different layers.

Response to the reviewers' comments

We would like to thank the reviewers for their careful evaluation of our manuscript. Their comments helped us improve the quality of this work.

Reviewer #1

A new design approach is presented that applies a fused deposition modeling process to create planar structures capable of out-of-plane deformation. By controlling the printing speed and incorporating multi-material printing, it is possible to obtain a variety of shapes covering negative to positive values of mean and Gaussian curvature. This is an interesting work, but some minor issues need to be addressed.

Remark 1.1. A sudden drop (between $h=1.5$ mm and $h=2$ mm) was observed from the β_2 curve in Figure 2b, and a more detailed explanation is needed to elucidate this phenomenon. Furthermore, in Figure 2b, are β_1 and β_2 an average value or were they tested only once?

We thank the reviewer for this observation. In Figure 2b, when the thickness of the specimens increased from 1.5 mm to 2 mm, a critical point was reached. At this point, the interplay between the specimens' thickness and the defects resulted from the printing process became increasingly evident. We have made the following modifications in the revised manuscript to explain this further:

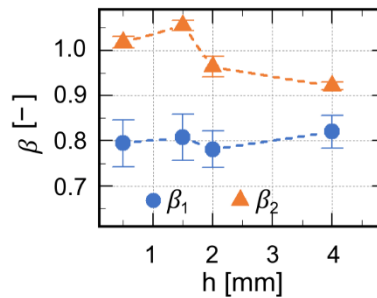
“To put this relationship into a broader perspective, we printed PLA disks with various thicknesses. For very thin disks (i.e., $h < 2$ mm), the contribution of cross-sectional stresses caused the specimens to fold or roll when triggered by external thermal energy (Figure 2a, and Figure S2 of the supplementary document). The overall bending deformation of the plates was optimum for a thickness of $h = 2$ mm, which is considered as the reference plate thickness throughout this study. For the specimens with larger thicknesses (i.e., $h = 4$ mm), the increase in the bending stiffness of the plates prevented them from fully bending (Figure 2a, and Figure S2 of the supplementary document). The expansion factors (β_1, β_2) of the disks were not constant among disks with different thicknesses, although these variations decreased with the out-of-plane thickness of the specimens (Figure 2b). These results were surprising, because we had not changed the printing parameters of the disks with different thicknesses. This can be attributed to changes in various factors, such as the change in the bending stiffness and the distribution of defects during the 3D printing process when changing the thickness of the disk. Furthermore, we 3D printed square-shaped specimens at speeds of 20 and 80 mm/s. The results showed that $\beta_2 \approx 1$ in the transverse direction, independent of the printing speed (Figure S1a of the supplementary document). To explain this behavior, we further analyzed the mechanical properties of the constituent PLA as well as the morphological features of the 4D printed disks.”

The relatively thin specimens (i.e., $h < 2$ mm) are more prone to bending due to a higher surface area-to-volume ratio and fewer printing defects, especially in their initial layers (Figure 2e–f). This results in β_2 exceeding 1. However, when the thickness reaches 2 mm, internal stresses and the defects generated during the printing process become more pronounced, reducing β_2 and limiting the bending tendency of the disk. The dominant factors here include increased bending stiffness and shrinkage in the printing direction (β_1). To provide a more detailed understanding of the observed phenomenon, we have added the following paragraph to the revised manuscript:

“To probe this relation, several disks of thicknesses $h = 2$ mm were printed from PLA with different speeds ranging between 20 mm/s and 80 mm/s (the printing speed was uniform for each specimen). Once the heat stimulus is applied, the disks deform into cones with the most acute one corresponding to the highest printing speed, in qualitative agreement with Equation (2) (Figure 1 c-d). We measured the longitudinal expansion coefficients of the specimens printed at different printing speeds (Figure 1c). Our experimental results confirmed that increasing the printing speed decreased the magnitude of the longitudinal expansion factor of the specimens (Figure 1c). This can be explained by the fact that increasing the printing speed results in elongated filaments with smaller diameters. Interestingly, the effective values measured for β_2 are not larger than 1 as expected at the scale of a filament. We interpret this observation by the presence of void defects between the deposited filaments as described later. We also found an excellent agreement between the experimentally determined cone angles and the cone angles predicted analytically using Equation (2) (Figure 1d, e).”

“The behavior of the 4D printed specimens is influenced by the distribution of micro-defects within the specimens. As illustrated in Figure 2a, the impact of non-uniform distribution of micro-defects across the thickness is more pronounced for thinner specimens (i.e., $h < 2$ mm) with a lower bending stiffness. These specimens are more likely to exhibit folding or rolling behaviors. Additionally, fewer defects and non-uniformities occur in the initial layers during the printing process (Figure 2e–f). These characteristics collectively result in greater radial expansion, yielding an expansion factor (β_2) greater than 1 (Figure 2b). However, when the specimen thickness reaches 2 mm, other factors such as in-plane stresses, bending stiffness, and printing-induced non-uniformities become more significant. This leads to reduced transverse expansion and a decrease in the β_2 value (Figure 2b). The specimens then become less susceptible to bending while shrinkage in the radial printing direction (β_1) becomes more dominant.”

Regarding the measurement of β_1 and β_2 , these expansion factors were experimentally determined and shown in Figure 2b of the revised manuscript. To ensure reliability, we conducted multiple tests and calculated average values. These experiments were performed three times for consistency. We have updated subfigure b in Figure 2 and have included error bars in the plots that indicate the standard deviation of the reported mean values.



Remark 1.2. More details about the computational modeling should be shown, especially the input of material parameters (including anisotropic thermal expansion) and loading conditions (temperature) in the temperature-displacement steady-state analysis.

We appreciate the reviewer’s comment about the details of our computational model. We used orthotropic thermal expansion coefficients to model the anisotropic thermal relaxation behavior of PLA. These coefficients, which were presented in Table S1 of the supplementary

document, were determined based on the experimental data and calculations discussed in the “Measurement of expansion factors” section. To incorporate temperature-dependent properties, we used temperature-dependent elastic moduli (*i.e.*, $E(T)$) which were based on our dynamic mechanical analysis (DMA). This approach enabled us to simulate how the stiffness of PLA changes as a function of temperature. We applied a uniform temperature load of 100 °C to replicate the shape transformations observed experimentally. These details have been further elaborated in the “Computational modeling” section.

“Measurement of expansion factors. We measured the expansion factors along the printing direction (β_1 = longitudinal expansion factor) and perpendicular to the printing direction (β_2 = transverse expansion factor) using Equation (2) (Figure 1b) for PLA specimens printed at different printing speeds (Figure 1c) and thicknesses (Figure 2b). Although the actual shape transformation is not, from a physics viewpoint, a thermal expansion effect, it is numerically expedient to model it through a standard heat expansion routine with orthotropic expansion coefficients. We extracted the α_1 and α_2 values from the longitudinal and transverse expansion coefficients (β_1 and β_2):

$$\alpha_i = \frac{\beta_i - 1}{\Delta T}, \quad i = 1, 2 \quad \Delta T = 80 \text{ }^\circ\text{C}$$

(3)

The parameter α_3 was measured by comparing the thickness of the samples before and after thermal actuation. We also assumed that TPU is an incompressible material and employed orthotropic thermal expansion coefficients to ensure that its volume did not change after being exposed to high temperatures (see Table S1 of the supplementary document).

Computational modeling. Finite element modeling was conducted using the commercial software suite Abaqus (Dassault Simulia, V6.14, USA). We used linear thermally-coupled brick elements with full integration points in three directions (C3D8T, Abaqus). We uniformly applied the temperature with a magnitude of 100 °C ($= T_{\text{ambient}} + \Delta T$) to perform a coupled temperature–displacement steady-state analysis. In order to mimic the anisotropic relaxation we observed above the glass transition temperature, we considered temperature-dependent elastic moduli ($E(T)$) and orthotropic thermal expansion coefficients as the material model in our computational models. *These values were obtained from experimental data and are presented in Tables S1 and S2 of the supplementary document.*

We applied a symmetric boundary condition which enabled us to model half of the disk. The center of the disk was fixed. The model was discretized using five elements in thickness and radial elements with a size of 700 μm . The imperfections were introduced into the computational models by assigning extremely low mechanical properties (*i.e.*, $E = 1 \text{ Pa}$) to certain elements of the disk to trigger the instabilities in the system after applying the load [54-56]. The imperfections were distributed systematically to imitate the same distribution patterns as seen in the μCT images. The porosity of the PLA specimens printed at 80 mm/s was increased in both radial and build directions (Figure 2e–f), assuming that the initial layer (20% of thickness) was effectively defect-free. The imperfections were, therefore, implemented every $\sim 2.1 \text{ mm}$ between $R_{\text{in}}/R \sim 30\%$ (this number can be $\sim 15\%$ for the top layers) and $R_{\text{in}}/R \sim 100\%$ (*i.e.*, the peripheral edge of the specimens) (Figure S3a of the supplementary document).

The sensitivity of the FE models to the distribution of the imperfections was analyzed computationally. We observed that the defects were not distributed uniformly at each layer (Figure 2d). We, therefore, implemented a non-symmetric distribution of the imperfections in the angular direction and examined the effects of varying the angle of the imperfection distribution (γ) (i.e., from 30° to 150°) on the shape-shifting behavior of the constructs. Our results showed that the imperfection distribution in the angular direction (γ) does not significantly affect the cone angle (θ) (Figure S3b of the supplementary document). We considered the distribution of imperfections with $\gamma = 120^\circ$ in our model. A good agreement was achieved between the proposed computational model and our experimental observations (Figure S3c of the supplementary)."

Remark 1.3. Are the material parameters in Tables S1 and S2 the ones actually measured in this study?

The material parameters listed in Tables S1 and S2 of the supplementary document correspond to the values used in our computational simulations and were experimentally measured in this study. Please also see our response to Remark 1.2.

Remark 1.4. Was the temperature-dependent elastic moduli of PLA determined by tensile experiments, or was the storage modulus from the DMA used directly as a substitute? If the latter, it is not rigorous.

We appreciate the reviewer's focus on the characterization of temperature-dependent mechanical properties in our study. We would like to clarify this point. Here, we employed complex moduli obtained from DMA tests, rather than exclusively using the storage modulus, to establish the temperature-dependent elastic moduli of PLA. These complex moduli, which include both storage (elastic) and loss (viscous) components, serve as indicators of a material's resistance to deformation. While using complex modulus data instead of tensile tests may appear as a simplification, it is important to note that DMA measurements are widely accepted for characterizing the mechanical properties of shape memory polymers such as PLA across varying temperatures [1]. This method was deliberately selected in our study to accurately capture the temperature-dependent behavior of PLA material, ensuring that our simulations closely aligned with our experimental observations. We hope that this explanation clarifies our methodology and confirms its appropriateness for our research objectives.

[1] Bodaghi, M., A. R. Damanpack, and W. H. Liao. "Adaptive metamaterials by functionally graded 4D printing." *Materials & Design* 135 (2017): 26-36.

Remark 1.5. The authors create "imperfections" by setting different printing speeds. Can the inevitable gaps between deposition lines in the FDM process be introduced as "imperfections"? We thank the reviewer for their comment. In the FDM process, the formation of "imperfections" is due to the gaps that are created between consecutive deposition lines. In an ideal setting, minimizing/eliminating these gaps is a common objective. However, these gaps are intrinsic to the FDM process and can substantially influence the mechanical properties and the overall performance of the printed objects. Here, we observed that varying the printing speed can be used as a tool to deliberately introduce and control these imperfections during the FDM 3D printing process. We have also characterized these imperfections by performing non-destructive imaging characterization (i.e., micro-CT scanning), to demonstrate their presence and distribution in the 3D printed structures.

Reviewer #2

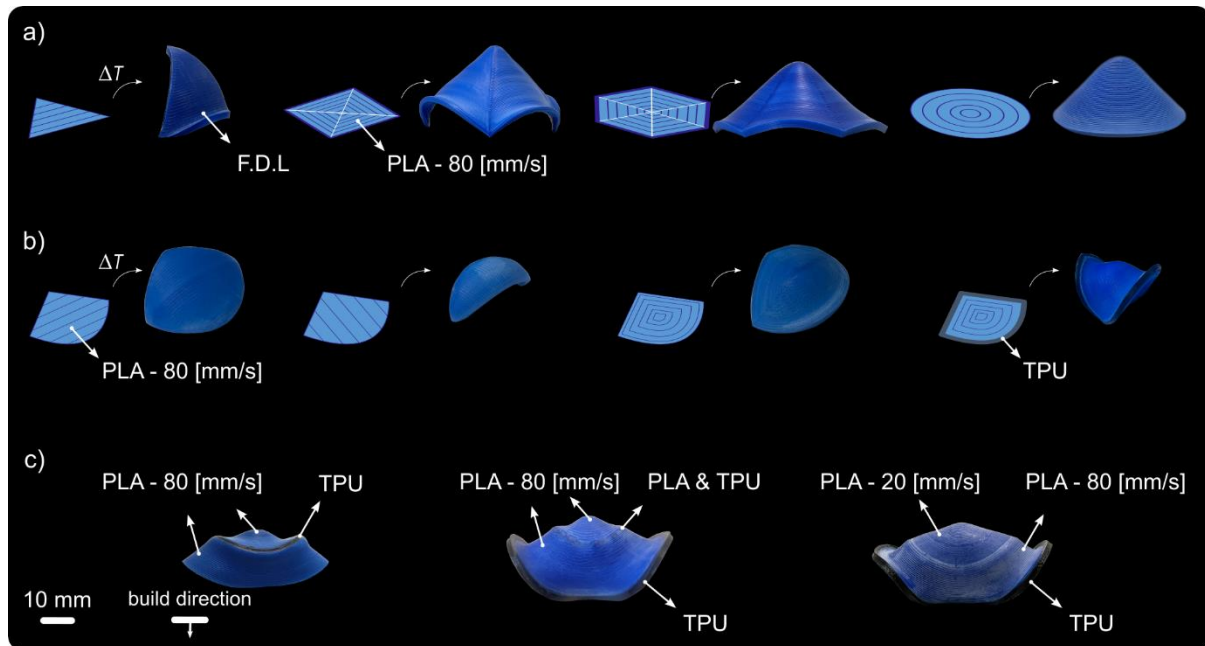
This paper utilized the combination of PLA material and other softer materials, and the disc bends into a smooth surface of various curvations by adjusting the area proportion of the two materials. Also, the disc structure can be deformed into a dome structure of different curvations as needed with applying different printing speeds to the two materials in the area. Moreover, the reverse bending disk and the positive bending disk can be combined, such as the structure composed of the dome structure below and the saddle-shaped curved structure above.

Remark 2.1. Only the influence on the change of the proportion of the two materials in the radial direction of the disk on the deformation is discussed, which should be further discussed in the axial direction. For example, the disk is divided into several layers with the same and uniform thickness, and whether the number of layers occupied by the two materials has an influence on the deformation effect should be included. What's more, the influence of different layers occupied by PLA material and TPU material on surface curvature shall be further refined.

We thank the reviewer for their comment. The rationale behind our choice to implement TPU in a radial distribution within the disks is twofold. First, creating a robust bond between TPU and PLA is challenging, especially when these materials are axially stacked. At very high printing speeds (e.g., 80 mm/s) and 100% cooling rates, we have observed issues related to the adhesion and delamination of the printed structures. Second, since TPU does not significantly deform when the disk is triggered by heat, placing TPU in this form will not have any contribution to the overall deformation of PLA. In another words, when the structure deforms, we observed two extreme behaviors from both materials (i.e., PLA tends to spontaneously deform while TPU does not) which can result in the separation of both materials at their interfaces. In the revised version, we have tried to expand the range of explored design options in some alternative ways by studying new designs for the radial distribution of TPU in combination with different printing speeds at radial segments of the 3D printed PLA disk (Figure S5c of the supplementary document). Such implementation has allowed us to achieve even more complex shapes with various curvatures. The following paragraph has been added to the revised manuscript.

“To further study the effects of the boundary conditions on the overall shape-shifting behavior of the specimens, we used multi-material 4D printing with a soft polymer (i.e., thermoplastic polyurethane or TPU) as the second material. The elastic modulus of TPU is an order of magnitude lower than that of PLA. It also does not exhibit the capability of storing residual stresses and relaxing them in the temperature range used in this study (i.e., $40\text{ }^{\circ}\text{C} < T < 100\text{ }^{\circ}\text{C}$) (Figure 2c). We segmented the disk into two regions (i.e., inner and outer). The inner region was printed with the highest speed (i.e., 80 mm/s) while the outer region was made of TPU (printing speed = 25 mm/s). TPU does not show any shape transformation when the specimens are heated. The shape transformation of the PLA part can, therefore, be tuned by the amount of the soft material printed around it (Figure 4a–left). These boundary effects also contributed to the formation of local curvatures in the 4D printed multi-material disks. When 40% of the disk was printed from TPU, the local curvatures were close to zero within the TPU part (i.e., no deformation) while a positive curvature (i.e., dome-like or spherical) appeared at the disk center (Figure 4a–right). Decreasing the size of the TPU to 10% extended the range of achievable Gaussian and mean curvatures towards more negative and positive values (Figure 4a–right). A comparable behavior was observed across various printing and TPU deposition patterns (Figures S1 and S5 of the supplementary document). We further demonstrated that the specific positioning of

TPU did not affect the overall curvature profile (Figure S5c of the supplementary document). For example, when the TPU ring was placed internally (i.e., in the inner ring), the global saddle-like curvature was achieved (Figures S5c-left of the supplementary document). Placing PLA atop the TPU in the middle ring (Figure S5c-middle of the supplementary document) affected the bending stiffness of the disk, resulting in diminished overall curvature. Hence, the synergy between multi-material printing and the strategic placement of imperfections effectively allows for the modulation of residual stresses and bending stiffnesses, thereby facilitating a wide range of curvature types (Figure S5c of the supplementary document).”



“**Figure S5:** The out-of-plane deformation in 2D structures made from different initial shapes (i.e., triangle with horizontal filament patterns, as well as square, hexagon, and circle with concentric filament deposition) showed similar dome-shape result after triggered by temperature (a). In these specimens, we used printing speed of 80 mm/s. We further combined these shapes (i.e., triangle and semi-circle) and 3D printed 2D planes with four different printing patterns including linear-horizontal, linear-vertical, concentric and the combination of concentric and multi-material (b). The printing pattern can significantly affect the out-of-plane results. We also showed how deposition of TPU can change the curvature that can be achieved during 4D printing (c). All specimens were 3D printed with an out-of-plane thickness of 2 mm. $V_{PLA}/V_{total} = 90\%$ was considered in multi-material specimens. The first deposited layers (F.D.L) are illustrated in (a–c).”

Remark 2.2. If it is possible, it’s better to further refine the area of the material in the disc, and select a variety of materials to distribute in various proportions in the radial and axial directions of the disc, so that the disc presents a gradient structure and can be deformed into a more complex curved surface structure with multiple gradients and curvations.

We thank the reviewer for their suggestion. In the revised manuscript, we have explored several new designs while combining the parameters, such as printing speed and multi-material deposition (please see our response to Remark 2.1). The implementation of functional gradients in the material using the FDM process is practically very challenging. While it is possible that extensive study and optimization would enable the fabrication of such structures using the

FDM process, it would likely require a dedicated study and is beyond the scope of the current study. We have, therefore, decided not to include that in our results.

Remark 2.3. In this paper, there is no 3D solid sample successfully printed by this design method for practical application, if it is possible to print a three-dimensional solid structure that realizes functional gradient characteristic utilizing the gradient structure.

We thank the reviewer for their comment. The specimens depicted in Figures 5a and b are 3D structures, which were all successfully 3D printed and tested. As previously mentioned, the incorporation of functional gradients in the material is not practically possible using the FDM processes. We have already incorporated and successfully tested the concept of gradients of the printing speed in our disks (see Figure 1g).

Reviewer #3

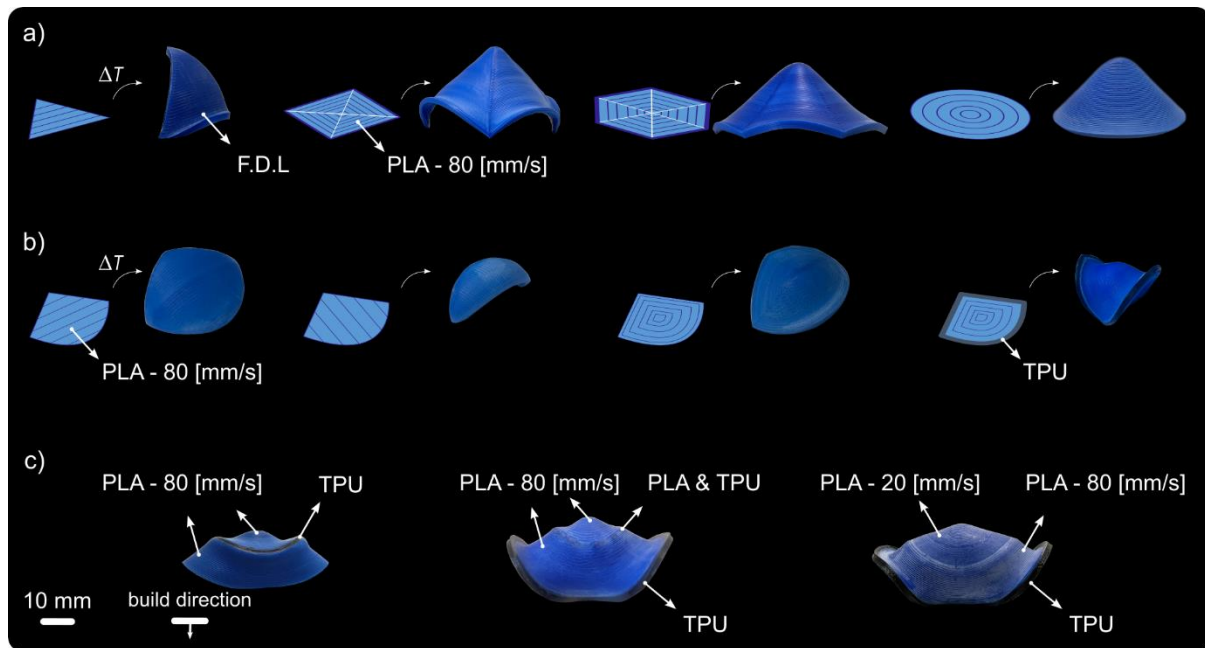
The authors present a methodology coupled with modelling of the deformation of FDM components, including those built from multi-materials. The following minor comments should be taken into account for this manuscript to be further considered.

Remark 3.1. Deformations and stress/strain distributions are influenced by the selected concentric rings printing path. So, what can the authors expect if other printing trajectories are selected?

We thank the reviewer for their comments. We agree that the choice of printing patterns can significantly influence the resulting deformations. The reason for selecting a concentric path as the printing pattern is twofold. Firstly, our aim was to establish an axisymmetric condition as an initial step in our experimental approach that is similar to our analytical analysis. Secondly, when dealing with a disk geometry and employing concentric printing, in-plane stresses tend to assume a more prominent role. To elucidate the effects of different printing patterns and initial shapes on the overall deformations of the 4D printed structures, we have conducted a series of new designs. These additional results have been incorporated into the revised manuscript and are detailed in the supplementary document.

“To further study the effects of the boundary conditions on the overall shape-shifting behavior of the specimens, we used multi-material 4D printing with a soft polymer (i.e., thermoplastic polyurethane or TPU) as the second material. The elastic modulus of TPU is an order of magnitude lower than that of PLA. It also does not exhibit the capability of storing residual stresses and relaxing them in the temperature range used in this study (i.e., $40\text{ }^{\circ}\text{C} < T < 100\text{ }^{\circ}\text{C}$) (Figure 2c). We segmented the disk into two regions (i.e., inner and outer). The inner region was printed with the highest speed (i.e., 80 mm/s) while the outer region was made of TPU (printing speed = 25 mm/s). TPU does not show any shape transformation when the specimens are heated. The shape transformation of the PLA part can, therefore, be tuned by the amount of the soft material printed around it (Figure 4a–left). These boundary effects also contributed to the formation of local curvatures in the 4D printed multi-material disks. When 40% of the disk was printed from TPU, the local curvatures were close to zero within the TPU part (i.e., no deformation) while a positive curvature (i.e., dome-like or spherical) appeared at the disk center (Figure 4a–right). Decreasing the size of the TPU to 10% extended the range of achievable Gaussian and mean curvatures towards more negative and positive values (Figure 4a–right). A comparable behavior was observed across various printing and TPU deposition patterns (Figures S1 and S5 of the supplementary document). We further demonstrated that the specific positioning of TPU did not affect the overall curvature profile (Figure S5c of the supplementary

document). For example, when the TPU ring was placed internally (i.e., in the inner ring), the global saddle-like curvature was achieved (Figures S5c-left of the supplementary document). Placing PLA atop the TPU in the middle ring (Figure S5c-middle of the supplementary document) affected the bending stiffness of the disk, resulting in diminished overall curvature. Hence, the synergy between multi-material printing and the strategic placement of imperfections effectively allows for the modulation of residual stresses and bending stiffnesses, thereby facilitating a wide range of curvature types (Figure S5c of the supplementary document).”



“**Figure S5:** The out-of-plane deformation in 2D structures made from different initial shapes (i.e., triangle with horizontal filament patterns, as well as square, hexagon, and circle with concentric filament deposition) showed similar dome-shape result after triggered by temperature (a). In these specimens, we used printing speed of 80 mm/s. We further combined these shapes (i.e., triangle and semi-circle) and 3D printed 2D planes with four different printing patterns including linear-horizontal, linear-vertical, concentric and the combination of concentric and multi-material (b). The printing pattern can significantly affect the out-of-plane results. We also showed how deposition of TPU can change the curvature that can be achieved during 4D printing (c). All specimens were 3D printed with an out-of-plane thickness of 2 mm. $V_{PLA}/V_{total} = 90\%$ was considered in multi-material specimens. The first deposited layers (F.D.L) are illustrated in (a–c).”

Remark 3.2. Why did the authors select this printing path?

We thank the reviewer for their comments. In addition to our response to Remark 3.1, we would like to provide further elaboration in response to this remark.

In the revised version of the manuscript, we have conducted additional experiments on square plates that were printed with both the minimum (i.e., 20 mm/s) and maximum (i.e., 80 mm/s) printing speeds. These new experiments have revealed two distinct deformation responses for these plates, substantiating the combined influence of defect distribution throughout the thickness and chosen printing patterns on the topic that we are exploring. Particularly, we have observed shrinkage in the printing direction and expansion in the transverse direction for the

specimens printed at lower printing speeds. This behavior starkly contrasts with the outcome for the specimens printed at the highest speed, which showed out-of-plane deformations.

Furthermore, the use of concentric pattern offered a high level of geometric symmetry, thereby simplifying both our experimental investigations and computational simulations. Symmetric structures inherently tend to be more predictable and easier to model, making them a suitable choice for our study. We have also demonstrated how a disk structure with concentric patterns can be shaped by sectors of linear patterns in Figure S5a of the supplementary document. This circular geometry with concentric patterns exhibited a more predictable shape.

We have also incorporated TPU in those 3D printed PLA square plates, and we have observed similar deformation as those observed in disk specimens (Figure S1 of the supplementary document).

The following paragraphs have been added to the revised manuscript:

“Furthermore, we 3D printed and tested square plates that were respectively printed at two distinct printing speeds: the minimum (i.e., 20 mm/s) and the maximum (i.e., 80 mm/s). The plate printed at the lower printing speed exhibited longitudinal shrinkage along the printing direction and transverse expansion (Figure S1a of the supplementary document). Importantly, in this case, no out-of-plane deformation was observed in the overall deformation. Indeed, since the direction of contraction remains parallel and the contraction rate is uniform, Gaussian curvature is not expected to occur [1]. In contrast, the plate printed at the higher printing speed exhibited an unexpected out-of-plane deformation, appearing as a bending feature (Figure S1a of the supplementary document). This observation highlighted that plates printed at a higher speed experience not only an in-plane stress but also a stress gradient through the plate thickness. The interplay between these two stress components contributes to different behavior when subjected to elevated temperatures. As a matter of fact, the layers printed at the vicinity of printer build-plate apparently accumulates less residual stress than the upper layers. As a consequence, standard bilayer effect tends to induce a concavity on the opposite side of the build-plate to the different structures that were printed with a uniform speed across the thickness [2]. Although this bending effect is not significant in the thicker specimens (beyond selecting the side where the concavity appears), bending is observed for thinner specimens (Figure S2 of the supplementary document).”

“We also further delved into the effects of printing patterns (Figure S1 of the supplementary document) and initial shape of the 2D plates (Figures S5a, and S5b of the supplementary document) on the overall shape of the 4D printed structures. Toward that end, we printed plates, as concentrically printed filaments, at a speed of 80 mm/s. When exposed to high temperatures, independent from the printing patterns and the initial shape of the plates, they showed a dome-like out-of-plane deformation (Figures S1b, S5a, and S5b of the supplementary document). When the multi-material approach was used (i.e., printing TPU at the boundaries of the plate regardless of the printing direction), the parts printed from TPU remained unaffected and created discontinuity at the boundaries of the plate. This led to similar negative Gaussian curvatures as observed in disks (Figures S1a-bottom, and S1b-bottom of the supplementary document).”

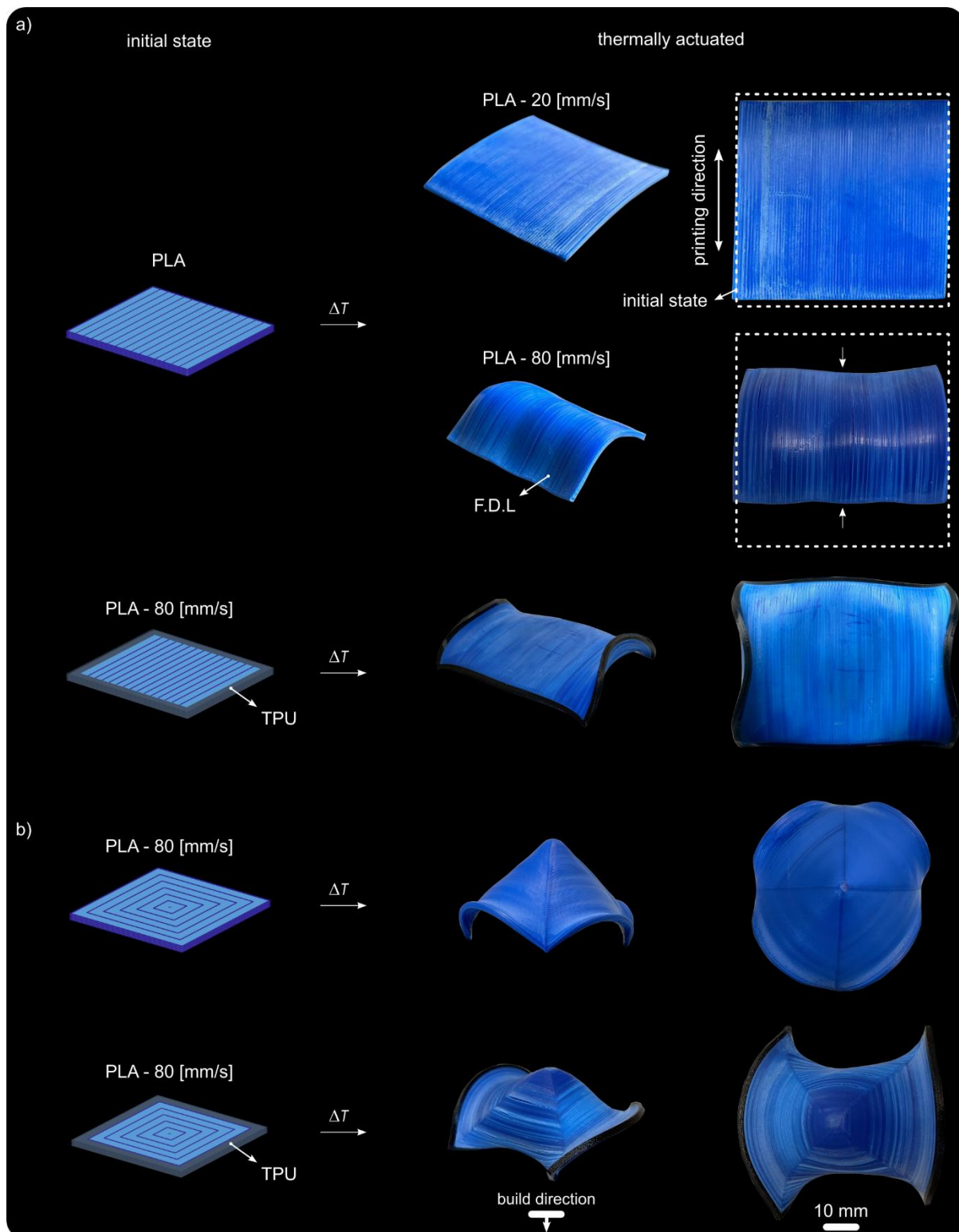


Figure S1. The effects of residual stresses positioning on the shape-shifting behavior of square-shaped structures. PLA square plates were 3D printed at speeds of 20 and 80 mm/s, using linear patterns, and incorporating TPU (a), as well as using concentric patterns with and without TPU (b). All the specimens were printed with a uniform thickness of 2 mm. When a multi-material printing approach was used, $V_{\text{PLA}}/V_{\text{total}} = 90\%$ was maintained. The first deposited layers (F.D.L) are illustrated in (a) and (b).

- [1] H. Aharoni, Y. Xia, X. Zhang, R.D. Kamien, S. Yang, Universal inverse design of surfaces with thin nematic elastomer sheets, *Proceedings of the National Academy of Sciences* 115(28) (2018) 7206-7211.
- [2] S. Timoshenko, Analysis of bi-metal thermostats, *Josa* 11(3) (1925) 233-255.

Remark 3.3. For the multi-material printed samples, In %, how much PLA and TPU were used? Discussion on different multi-material strategies could also enhance the current version, e.g., different materials in different layers.

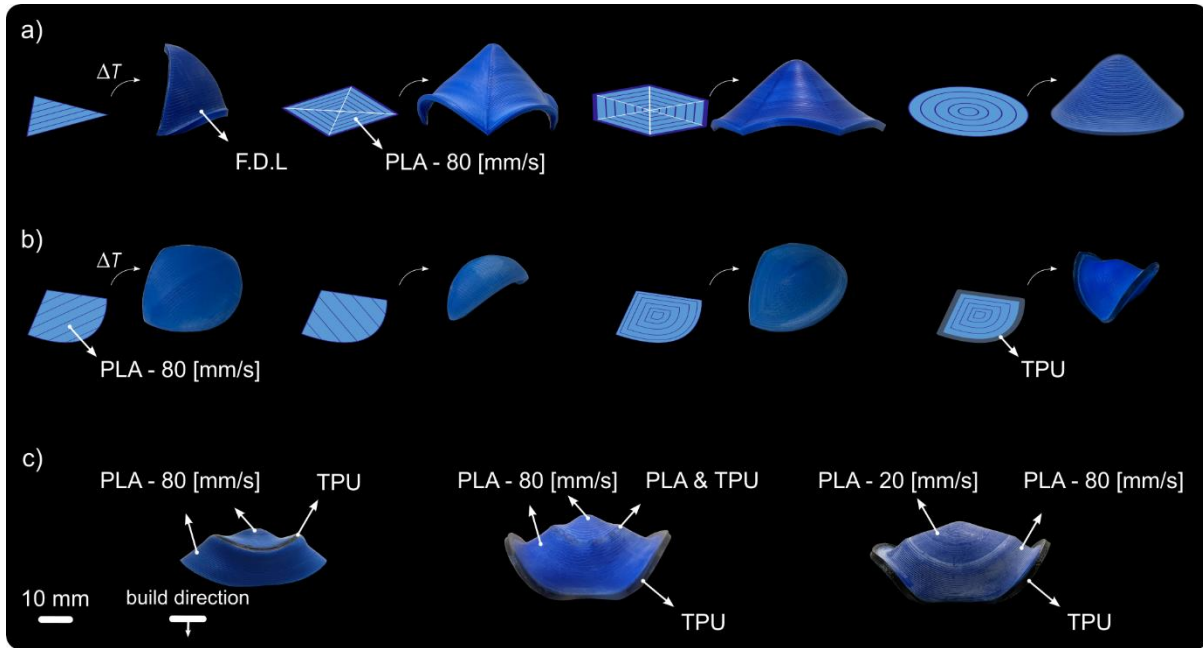
We thank the reviewer for bringing this into our attention. We used a ratio of $V_{PLA}/V_{total} = 90\%$ for our multi-material printed specimens. This ratio has been used throughout our study, unless otherwise stated. We have added the following clarification to the “4D printing” section:

“In the specimens shown in Figures 5b, we employed the printing strategy described in sub-Figure 5a to print specimens 1 and 2 on top of each other. To print the specimens in one step, we placed an adhesive sheet (Tesa 4438 Blue Tape) between both disks in the middle of the printing process. Only a small section of the center ($R_{in}/R \sim 5\%$) was not covered by the adhesive sheet to connect the specimens. For the multi-material printed specimens, a composition ratio of $V_{PLA}/V_{total} = 90\%$ was used. This ratio was maintained constant unless otherwise stated.”

Regarding the discussion on the use of different multi-material strategies, we agree that exploring various material combinations and layering techniques can further enhance the capabilities of multi-material FDM printing. However, it is important to note that multi-material FDM printing comes with certain limitations, such as challenges in achieving reliable bonding between different materials and potential delamination issues in a single print. In response to the reviewer’s suggestion, we have explored and demonstrated the potential of combining material positioning imperfections with multi-material approaches in our study (Figures S5c of the supplementary document). By modifying the deposition of the TPU material within the disk, printing PLA on top of TPU in the inner ring, and designing specific structures that incorporate both concepts, we have showcased how these strategies can create even more complex deformations.

“To further study the effects of the boundary conditions on the overall shape-shifting behavior of the specimens, we used multi-material 4D printing with a soft polymer (i.e., thermoplastic polyurethane or TPU) as the second material. The elastic modulus of TPU is an order of magnitude lower than that of PLA. It also does not exhibit the capability of storing residual stresses and relaxing them in the temperature range used in this study (i.e., $40\text{ }^\circ\text{C} < T < 100\text{ }^\circ\text{C}$) (Figure 2c). We segmented the disk into two regions (i.e., inner and outer). The inner region was printed with the highest speed (i.e., 80 mm/s) while the outer region was made of TPU (printing speed = 25 mm/s). TPU does not show any shape transformation when the specimens are heated. The shape transformation of the PLA part can, therefore, be tuned by the amount of the soft material printed around it (Figure 4a–left). These boundary effects also contributed to the formation of local curvatures in the 4D printed multi-material disks. When 40% of the disk was printed from TPU, the local curvatures were close to zero within the TPU part (i.e., no deformation) while a positive curvature (i.e., dome-like or spherical) appeared at the disk center (Figure 4a–right). Decreasing the size of the TPU to 10% extended the range of achievable Gaussian and mean curvatures towards more negative and positive values (Figure 4a–right). A comparable behavior was observed across various printing and TPU deposition patterns (Figures S1 and S5 of the

supplementary document). We further demonstrated that the specific positioning of TPU did not affect the overall curvature profile (Figure S5c of the supplementary document). For example, when the TPU ring was placed internally (i.e., in the inner ring), the global saddle-like curvature was achieved (Figures S5c-left of the supplementary document). Placing PLA atop the TPU in the middle ring (Figure S5c-middle of the supplementary document) affected the bending stiffness of the disk, resulting in diminished overall curvature. Hence, the synergy between multi-material printing and the strategic placement of imperfections effectively allows for the modulation of residual stresses and bending stiffnesses, thereby facilitating a wide range of curvature types (Figure S5c of the supplementary document).”



“**Figure S5:** The out-of-plane deformation in 2D structures made from different initial shapes (i.e., triangle with horizontal filament patterns, as well as square, hexagon, and circle with concentric filament deposition) showed similar dome-shape result after triggered by temperature (a). In these specimens, we used printing speed of 80 mm/s. We further combined these shapes (i.e., triangle and semi-circle) and 3D printed 2D planes with four different printing patterns including linear-horizontal, linear-vertical, concentric and the combination of concentric and multi-material (b). The printing pattern can significantly affect the out-of-plane results. We also showed how deposition of TPU can change the curvature that can be achieved during 4D printing (c). All specimens were 3D printed with an out-of-plane thickness of 2 mm. $V_{PLA}/V_{total} = 90\%$ was considered in multi-material specimens. The first deposited layers (F.D.L) are illustrated in (a–c).”

8th Jan 24

Dear Dr Mirzaali,

Your manuscript titled "Curvature tuning through defect-based 4D printing" has now been seen again by our referees, whose comments appear below. Reviewer #3 has also kindly looked into the issues raised by Reviewer #2, as the latter was not available to look at the revised manuscript. In light of the referees' advice, I am delighted to say that we are happy, in principle, to publish a suitably revised version in Communications Materials under the open access CC BY license (Creative Commons Attribution v4.0 International License).

We therefore invite you to edit your manuscript to comply with our journal policies and formatting style, in order to maximise the accessibility and therefore the impact of your work.

EDITORIAL REQUESTS

* Your manuscript should comply with our policies and format requirements, detailed in our style and formatting guide (<https://www.nature.com/documents/commsj-phys-style-formatting-guide-accept.pdf>).

* Please edit your manuscript according to the editorial requests in the attached table, and outline revisions made in the right hand column. If you have any questions or concerns about any of our requests, please do not hesitate to contact me. It is important that each request be addressed in order to avoid delays in accepting your manuscript. Please upload the completed table with your manuscript files as a Related Manuscript file.

* The editorial requests table also includes a full list of the files that must be provided upon resubmission. Please upload your files according to this table.

* An updated editorial policy checklist that verifies compliance with all required editorial policies must be completed and uploaded with the revised manuscript. All points on the policy checklist must be addressed; if needed, please revise your manuscript in response to these points. Please note that this form is a dynamic 'smart pdf' and must therefore be downloaded and completed in Adobe Reader. Clicking this link will download a zip file containing the pdf.

Editorial policy checklist: <https://www.nature.com/documents/nr-editorial-policy-checklist.zip>

OPEN ACCESS

Communications Materials is a fully open access journal. Articles are made freely accessible on publication under a [CC BY](http://creativecommons.org/licenses/by/4.0) license (Creative Commons Attribution 4.0 International License). This license allows maximum dissemination and re-use of open access materials and is preferred by many research funding bodies.

For further information about article processing charges, open access funding, and advice and support from Nature Research, please visit <https://www.nature.com/commsmat/about/open-access>

RESUBMISSION

At acceptance, you will be provided with instructions for completing this CC BY license on behalf of all authors. This grants us the necessary permissions to publish your paper. Additionally, you will be asked to declare that all required third party permissions have been obtained, and to provide billing information in order to pay the article-processing charge (APC).

Please use the following link to submit your revised files:

[link redacted]

** This url links to your confidential home page and associated information about manuscripts you may have submitted or be reviewing for us. If you wish to forward this email to co-authors, please delete the link to your homepage first **

We hope to hear from you within two weeks; please let us know if the process may take longer.

Best regards,
Aldo

Dr Aldo Isidori
Senior Editor
Communications Materials

REVIEWERS' COMMENTS:

Reviewer #1 (Remarks to the Author):

The authors have revised the manuscript as suggested. The reviewer recommends that this version be accepted.

Reviewer #3 (Remarks to the Author):

Authors have addressed my comments and those of reviewer 2 satisfactorily.